Available online at www.sciencedirect.com

ScienceDirect

Ceramics International 34 (2008) 1573–1577

CERAMICS INTERNATIONAL

www.elsevier.com/locate/ceramint

Electrical properties and microstructure of Y-doped $BaTiO_3$ ceramics prepared by high-energy ball-milling

K. Park [a], J.-G. Kim [b,*], K.-J. Lee [c], W.S. Cho [c], W.S. Hwang [c]

[a] Department of Advanced Materials Engineering, Sejong University, Seoul, 143-747, Republic of Korea
[b] Inorganic Chemistry Examination Team, Korean Intellectual Property Office, Daejeon, 302-701, Republic of Korea
[c] School of Materials Science and Engineering, Inha University, Incheon, 402-751, Republic of Korea

Received 10 February 2006; received in revised form 3 March 2006; accepted 6 April 2006

Abstract

The effects of corn-starch content and high-energy ball-milling time on the microstructure and electrical properties of porous Y-doped (Ba, Sr)TiO_3 samples were investigated. All the (Ba, Sr)TiO_3 samples at room temperature crystallized in the tetragonal structure and the crystal structure was independent of the corn-starch content and ball-milling time. We found that the corn-starch additive and the ball-milling time affected the microstructure and the electrical properties. The (Ba, Sr)TiO_3 samples exhibited a large PTCR jump ($>10^5$) due to the high porosity. The PTCR jump of the samples increased with increasing corn-starch content, while it decreased with increasing ball-milling time. In addition, the resistivity increased with increasing corn-starch content, while it decreased with increasing ball-milling time.

Keywords: B. Porosity; PTCR; Porous ceramics; High-energy ball-milling; Corn-starch

1. Introduction

Polycrystalline barium titanate ($BaTiO_3$) exhibits a positive temperature coefficient of resistance (PTCR) characteristics [1–6]. The characteristics involve a substantial non-linear change of resistivity when the temperature reaches the Curie temperature (T_c) [7–17]. Several models have been developed to explain the PTCR characteristics [8,9,11,13]. One of the most recognized models is the Heywang's model [8,11]. The model is based on the formation of a potential barrier at the grain boundaries. This model has been extended by Jonker [9], who took into account of the influence of the polarization on the resistivity below the Curie temperature. This model is termed the Heywang–Jonker model. The PTCR characteristics provide wide applications such as color TV degausser, motor starter, self-regulating heaters, overcurrent limiters and so on [14]. Various fabrication techniques have been investigated to improve the PTCR characteristics. One of the techniques is to fabricate the porous $BaTiO_3$-based ceramics [12]. To date, porous $BaTiO_3$-based ceramics have been prepared with the incorporation of graphite, borides, silicides, carbides, partially oxidized Ti powders, polyethylene glycol and graphite to $BaTiO_3$ [14–18]. It can be considered that the composition and fabrication processes affect the microstructure and the PTCR characteristics in the porous ceramics. In this study, the effects of the corn-starch content and high-energy ball-milling time on the microstructure and electrical properties of the porous ceramics have been investigated.

2. Experimental procedure

Porous $BaTiO_3$-based ceramics, called (Ba, Sr)TiO_3, were fabricated by the addition of corn-starch (0–15 wt.%). Commercially available high-purity (Ba, Sr)TiO_3 powders containing 25 mol% SrO and 0.2 mol% Y_2O_3 (Toho Titanium Co. Ltd., Japan) were used. The mean particle size and ferroelectric Curie temperature of the powders were 0.7 μm and 61 °C, respectively. A mixture of the corn-starch (Shinyo Pure Chemicals Co. Ltd., Japan) and the Y-doped (Ba, Sr)TiO_3 powders was ball-milled in planetary mill (Fritsch, Germany) with ethanol media for 1–20 h using ZrO_2 balls (Ø 2 mm). And then the mixed powders were dried at 100 °C for 4 h. The dried

---

* Corresponding author. Tel.: +82 42 481 8304; fax: +82 42 472 3534.
E-mail address: iamjgkim@hanmail.net (J.G. Kim).

0272-8842/$34.00 © 2006 Elsevier Ltd and Techna Group S.r.l. All rights reserved.
doi:10.1016/j.ceramint.2006.04.007

Table 1
Summary of the samples obtained in this study

Corn-starch (wt.%)	Ball-milling time (h)	Sample
0	1	C0
5	1	C5
10	1	C10
15	1	C15
20	1	C20
15	1	1H (C15)
15	5	5H
15	10	10H
15	15	15H
15	20	20H

powders were compacted by die-pressing at 40 MPa to prepare the green compacts (15 mm × 12 mm × 7 mm). The green compacts were sintered at 1350 °C for 1 h in air. The samples obtained in this study are summarized in Table 1. The microstructure and crystal structure of the as-fabricated Y-doped (Ba, Sr)TiO_3 samples were analyzed by the scanning electron microscopy (SEM: S-4200, Hitachi) and the X-ray diffraction (XRD: PW-1710, Philips), respectively. The average grain size and porosity or pore size of the samples were estimated using the line-intersection method and the mercury porosimeter, respectively. The electrical resistance was measured with a digital multi-meter under air atmosphere. Capacitance–voltage (*C*–*V*) characteristics were measured with an impedance analyzer at room temperature at a frequency of 10 kHz in order to calculate the donor concentration of grains and the electrical potential barrier of grain boundaries.

3. Results and discussion

Fig. 1 shows the relationship between the electrical resistivity and temperature for samples C0–C20, indicative of PTCR characteristics. All samples show a large PTCR jump ($>10^5$). The electrical resistivity and the PTCR jump ($\rho_{max}/\rho_{25^\circ C}$) increased with increasing corn-starch content. For example, the room-temperature resistivities of samples C0, C10 and C20s are 31.8, 46.7 and 189 Ω cm, respectively, and the PTCR jumps of samples C0, C10 and C15 are 3.03×10^5, 9.10×10^5 and 9.14×10^5, respectively. Since the high-temperature (200–250 °C) electrical resistivity of sample

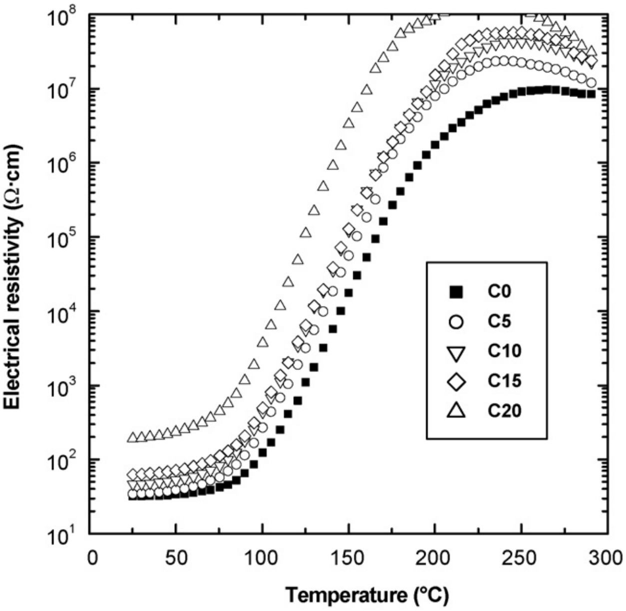

Fig. 1. Electrical resistivity as a function of temperature for samples C0–C20.

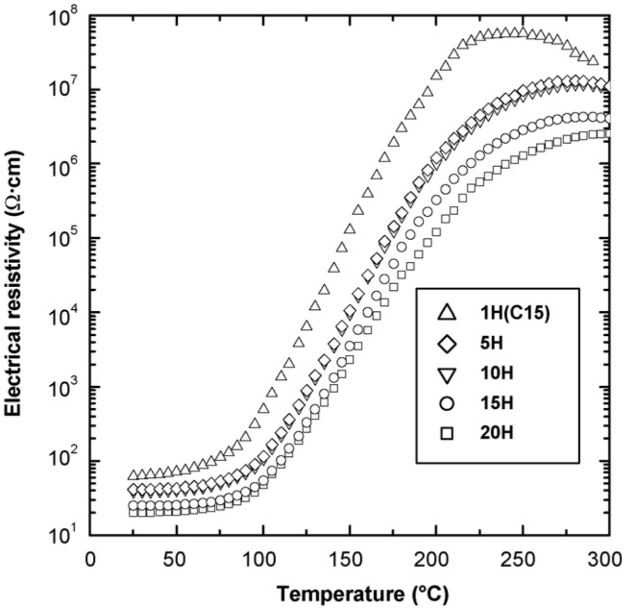

Fig. 2. Electrical resistivity as a function of temperature for samples 1H–20H.

Table 2
Porosity, average pore size, average grain size, room-temperature electrical resistivity ($\rho_{25^\circ C}$), maximum electrical resistivity (ρ_{max}), PTCR jump, donor concentration of grains and electrical potential barrier of grain boundaries at 25 °C for all the samples

Sample	Porosity (%)	Average pore size (μm)	Average grain size (μm)	$\rho_{25^\circ C}$ (Ω cm)	ρ_{max} (Ω cm)	PTCR jump ($\rho_{max}/\rho_{25^\circ C}$)	Donor concentration of grains (N_d, #/cm^3)	Electrical potential barrier of grain boundaries (Φ, eV)
C0	7.18	0.28	6.71	3.18×10	9.63×10^6	3.03×10^5	5.12×10^{18}	0.005
C5	12.45	0.85	6.52	3.43×10	2.35×10^7	6.85×10^5	4.77×10^{18}	0.006
C10	15.15	1.37	6.35	4.67×10	4.25×10^7	9.10×10^5	4.62×10^{18}	0.007
C15	17.59	2.38	5.94	6.26×10	5.72×10^7	9.14×10^5	4.53×10^{18}	0.011
C20	20.57	3.12	5.66	1.89×10^2	$>1.00 \times 10^8$	$>5.29 \times 10^5$	4.29×10^{18}	0.029
1H (C15)	17.59	2.38	5.94	6.26×10	5.72×10^7	9.14×10^5	4.53×10^{18}	0.011
5H	16.21	1.81	6.21	4.16×10	1.31×10^7	3.14×10^5	4.61×10^{18}	0.007
10H	15.19	1.46	6.65	3.85×10	1.17×10^7	3.04×10^5	4.95×10^{18}	0.006
15H	13.83	0.90	6.81	2.51×10	4.26×10^6	1.69×10^5	5.29×10^{18}	0.004
20H	10.45	0.34	7.03	1.99×10	2.53×10^6	1.27×10^5	5.46×10^{18}	0.003

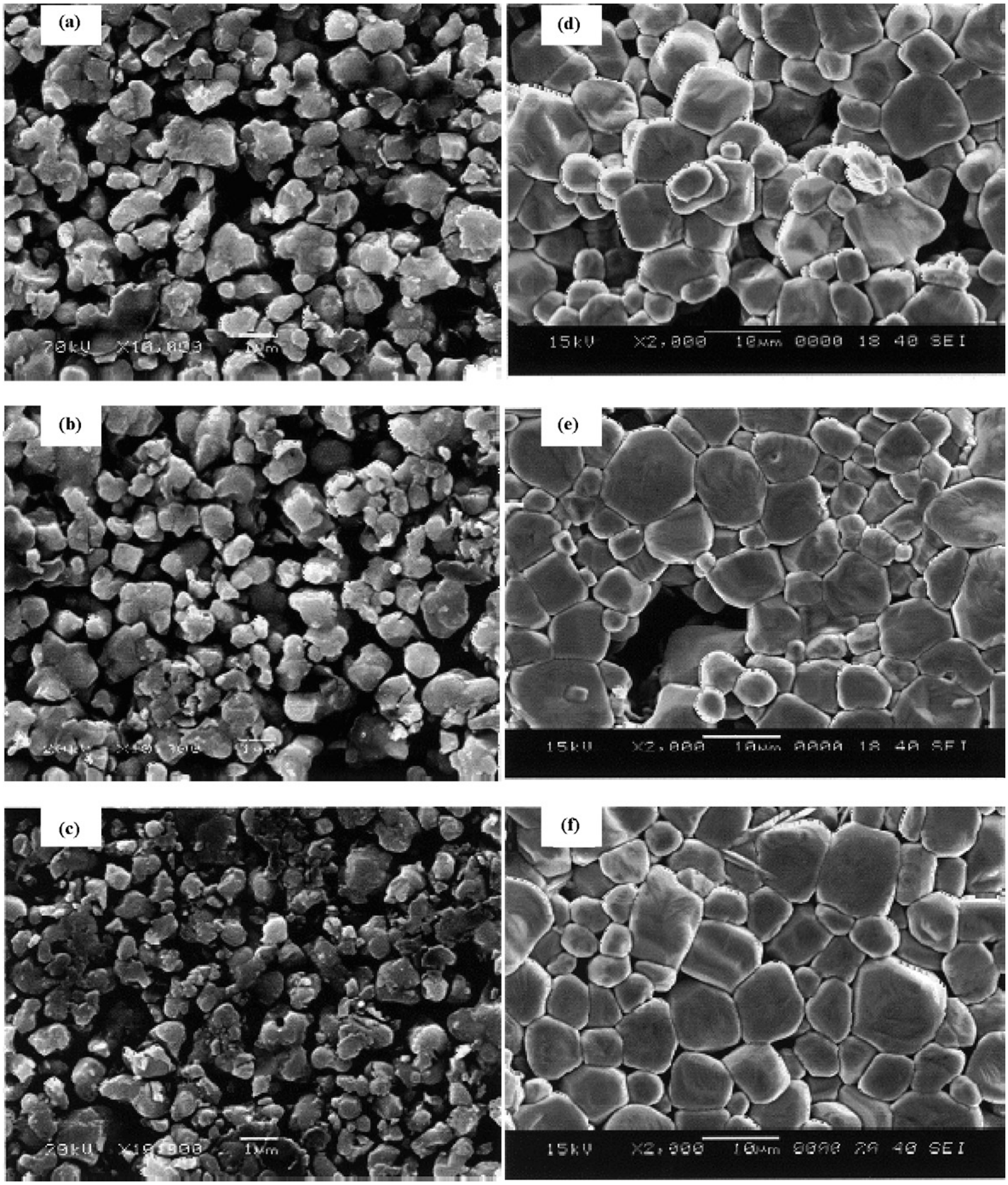

Fig. 3. SEM micrographs of the mixed powders and the fractured surfaces for samples 5H (a, d), 10H (b, e) and 20H (c, f).

C20 is higher than the measuring limit (10^8 Ω cm) of the multimeter used, it cannot be measured and is not seen in this figure. Sample C15 shows the highest PTCR jump (9.14×10^5) and sample C20 shows the highest room-temperature resistivity (189 Ω cm) due to its high porosity. In order to reduce the resistivity of the samples, we tried to decrease the porosity by increasing the ball-milling time.

Fig. 2 shows the electrical resistivity as a function of temperature for samples 1H–20H ball-milled for 1–20 h. The resistivity and the PTCR jump of all the samples decreased with increasing ball-milling time. For example, the room-temperature resistivities of samples 5H, 10H and 20H are 41.6, 38.5 and 19.9 Ω cm, respectively, and the PTCR jumps of samples 5H, 10H and 20H are 3.14×10^5, 3.04×10^5 and 1.27×10^5, respectively. In order to understand the variation in the resistivity of the samples depending on the corn-starch content and ball-milling time, we investigated the average grain size, porosity, average pore size, donor concentration of grains and electrical barrier height of grain boundaries for the samples.

Table 2 shows the porosity, the average grain size and the average pore size in all the samples. It is seen that with increasing corn-starch content, the porosity and average pore size increased because the added corn-starches acted as sites of the pore generation. The pores can be formed by the burning-out of corn-starches during sintering. Also, the grain size decreased as the corn-starch content increased due to the pore pinning effect. On the other hand, with increasing ball-milling time, the porosity and average pore size decreased and the grain size increased. For example, the SEM micrographs of the mixed powders and the fractured surfaces for the samples 5H, 10H and 20H ball-milled for 5–20 h are shown in Fig. 3. The average sizes of the mixed powders for samples 5H, 10H and 20H are 0.92, 0.72 and 0.64 μm, respectively. The powders with higher uniformity and narrower size distribution were obtained with increasing ball-milling time. Moreover, the porosities of samples 5H, 10H and 20H are 16.21, 15.19 and 10.45% respectively, and the average grain sizes of samples 5H, 10H and 20H are 6.21, 6.65 and 7.03 μm, respectively.

The capacitance-applied voltage variations at room temperature for samples C0, C10 and C20 are shown in Fig. 4. We calculated the donor concentration of grains and the electrical potential barrier of grain boundaries from the slope of the line and the intercept of the line on the voltage axis, respectively, as well as the equation proposed by Mukae et al. [19]. Table 2 shows the calculated donor concentration of grains and the electrical potential barrier of grain boundaries for all the samples. One can see that the donor concentration of grains for the samples did not change noticeably, but that the electrical barrier height of grain boundaries increased and decreased, respectively, with increases in corn-starch content and ball-milling time. An increase in the electrical barrier height of grain boundaries is mainly caused by the oxidation of grain boundaries. Oxygen is adsorbed at the grain boundaries during sintering in air to oxidize the grain boundaries. The porous ceramics are more favorable to oxidize grain boundaries, in comparison with dense ones [13,20,21].

From Table 2, an increase in the resistivity with increasing corn-starch content is mainly attributed to the increase in the electrical barrier height of the grain boundaries and partly to the increase in porosity and the decrease in the grain size. In addition, a decrease in the resistivity with increasing ball-milling time is due mainly to the decrease in the electrical barrier height of the grain boundaries and partly to the decrease in porosity and the increase of the grain size. Besides, it is important to note that the PTCR jump substantially increased with increasing porosity, which can be explained by the barrier model proposed by Heywang [8,11].

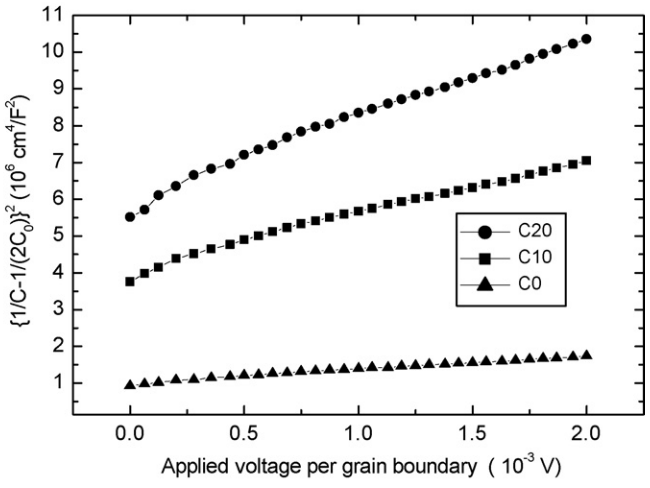

Fig. 4. Capacitance-applied voltage relation at room temperature for samples C0, C10 and C20.

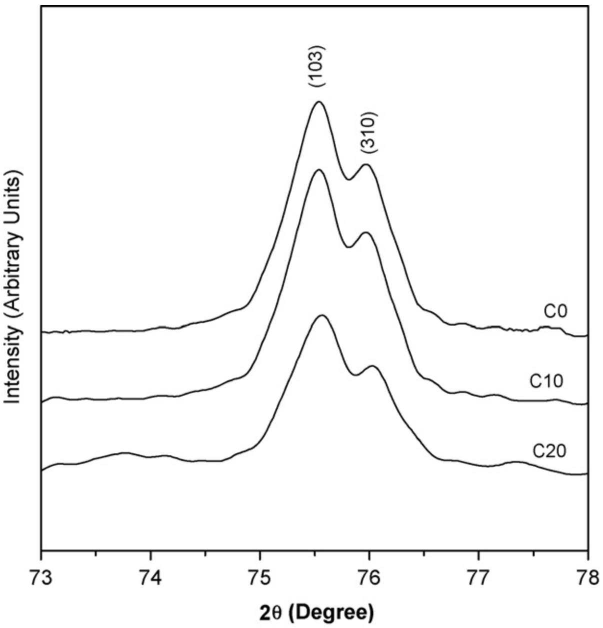

Fig. 5. XRD patterns measured at room temperature for samples C0, C10 and C20.

In order to investigate the effects of the corn-starch content and ball-milling time on the crystal structure, XRD analysis was performed with all the samples. It is difficult to identify the tetragonal and cubic phases in the (Ba, Sr)TiO_3 samples since the lattice parameters of the two phases are quite similar. Thus, the crystal structure of the samples was analyzed at high angles. The XRD patterns measured at room temperature for samples C0, C10 and C20 are shown in Fig. 5. All the samples crystallized in the tetragonal structure. The (1 0 3) and (3 1 0) peaks of the tetragonal phase are located at $2\theta = 75.51^\circ$ and 76.14°, respectively. The two peaks are slightly shifted towards higher angles compared with $BaTiO_3$ because of the substitution of Sr for the Ba site in the (Ba, Sr)TiO_3. The ionic radii of Sr and Ba atoms are 1.16 and 1.35 μm, respectively [22]. Also, the crystal structure of the (Ba, Sr)TiO_3 samples ball-milled for 5–20 h was basically the same as that of Fig. 5 (not shown here). These results suggest that the crystal structure of the (Ba, Sr)TiO_3 samples at room temperature is independent of the corn-starch content and ball-milling time. No secondary phase like carbon was detected.

4. Conclusions

Porous Y-doped (Ba, Sr)TiO_3 samples were prepared by adding corn-starch (0–15 wt.%) and their microstructure and electrical property were investigated. All the (Ba, Sr)TiO_3 samples at room temperature crystallized in the tetragonal structure and the crystal structure was independent of the corn-starch content and ball-milling time. With increasing corn-starch content, the porosity and average pore size increased and the grain size decreased. With increasing ball-milling time, the porosity and the average pore size decreased and the grain size increased. High porosity was responsible for a large PTCR jump ($>10^5$). As the corn-starch content increased, the resistivity also increased. This was attributed mainly to the increase in the electrical barrier height of the grain boundaries and partly to the increase in porosity and the decrease in the grain size. In addition, as the ball-milling time increased, the resistivity decreased. This was mainly due to the decrease in the electrical barrier height of grain boundaries and partly to the decrease in porosity and the increase in the grain size.

Acknowledgement

This work was supported by Inha University Research Grant.

References

[1] H. Nagamoto, H. Kagotani, T. Okubo, Positive temperature coefficient resistivity in $Ba_{1-x}Sr_xPb_{1+y}O_{3-\delta}$ ceramics, J. Am. Ceram. Soc. 76 (1993) 2053–2058.

[2] H. Emoto, J. Hojo, Sintering and dielectric properties of $BaTiO_3$-Ni composite ceramics, J. Ceram. Soc. Jpn. 100 (1992) 555–559.

[3] I.C. Ho, Semiconducting barium titanate ceramics prepared by boron-containing liquid-phase sintering, J. Am. Ceram. Soc. 77 (1994) 829–832.

[4] I.C. Ho, H.L. Hsieh, Influence of potassium on preparation and performance of PTC resistors, J. Am. Ceram. Soc. 76 (1993) 2385–2388.

[5] H.F. Cheng, T.F. Lin, C.T. Hu, Effect of sintering aids on microstructures and PTCR characteristic of $(Sr_{0.2}Ba_{0.8})TiO_3$ ceramics, J. Am. Ceram. Soc. 76 (1993) 827–832.

[6] B.C. Lacourse, V.R.W. Amarakoon, Characterization of the firing schedule for positive temperature coefficient of resistance $BaTiO_3$, J. Am. Ceram. Soc. 78 (1995) 3352–3356.

[7] O. Saburi, Semiconducting bodies in the family of barium titanates, J. Am. Ceram. Soc. 44 (1961) 54–63.

[8] W. Heywang, Semiconducting barium titanate, J. Mater. Sci. 6 (1971) 1214–1226.

[9] G.H. Jonker, Some aspects of semiconducting barium titanate, Solid State Electron. 7 (1964) 895–903.

[10] J. Daniels, K.H. Hardtl, R. Wernike, The PTC effect of barium titanate, Philips Tech. Rev. 38 (1978/1979) 73–82.

[11] W. Heywang, Resistivity anomaly in doped barium titanate, J. Am. Ceram. Soc. 47 (1964) 484–490.

[12] M. Kuwabara, Effect of microstructure on the PTCR effect in semiconducting barium titanate ceramics, J. Am. Ceram. Soc. 64 (1981) 639–644.

[13] M. Kuwabara, Influence of stoichiometry on the PTCR effect in porous barium titanate ceramics, J. Am. Ceram. Soc. 64 (1981) C170–C171.

[14] S.-M. Su, L.-Y. Zhang, H.-T. Sun, X. Yao, Preparation of porous $BaTiO_3$ PTC thermistors by adding graphite porosifiers, J. Am. Ceram. Soc. 77 (1994) 2154–2156.

[15] T.R. Shrout, D. Moffatt, W. Huebner, Composite PTCR thermistors utilizing conducting borides, silicides, and carbide powders, J. Mater. Sci. 26 (1991) 145–154.

[16] J.-G. Kim, W.-S. Cho, K. Park, PTCR characteristics in porous (Ba,Sr)-TiO_3 ceramics produced by adding partially oxidized Ti powders, Mater. Sci. Eng. B 77 (2000) 255–260.

[17] K. Park, J.-G. Kim, J. Kim, W.-S. Cho, Microstructure and electrical properties of porous $(Ba,Sr)TiO_3$ ceramics, Mater. Sci. Eng. B 88 (2002) 9–13.

[18] K. Park, Characteristics of porous $BaTiO_3$-based PTC thermistors fabricated by adding graphite powders, Mater. Sci. Eng. B 107 (2004) 19–26.

[19] K. Mukae, K. Tsuda, I. Nagasawa, Capacitance-vs-voltage characteristics of ZnO varistors, J. Appl. Phys. 50 (1979) 4475–4476.

[20] T. Takahashi, Y. Nakano, N. Ichinose, Influence of reoxidation on PTC effect of porous $BaTiO_3$, J. Ceram. Soc. Jpn. 98 (1990) 879–884.

[21] M. Kuwabara, Determination of the potential barrier height in barium titanate ceramics, Solid State Electron. 27 (1984) 929–935.

[22] S. Naka, S. Hayakawa, Electro-Ceramics, Ohmu-sha, Tokyo, Japan, 1986, p. 36.